

HARD EXCLUSIVE ELECTROPRODUCTION OF RESONANT AND  
NON-RESONANT PION PAIRS AT HERMES

ALEXANDER BORISSOV  
on behalf of the HERMES collaboration

*Department of Physics and Astronomy, University of Glasgow, Glasgow, G128QQ,  
United Kingdom*

Received 27 October 2003; Accepted 30 August 2004  
Online 22 November 2004

A selection of recent HERMES results is presented on the hard exclusive electroproduction of resonant and non-resonant  $\pi^+\pi^-$  pairs. The ratio of  $\rho^0$  electroproduction cross sections per nucleon on  $^{14}\text{N}$  as compared to that on  $^1\text{H}$ , known as the nuclear transparency, was found to increase (decrease) with increasing coherence length for coherent (incoherent)  $\rho^0$  electroproduction. For a fixed coherence length, a rise of the nuclear transparency with  $Q^2$  is observed for both coherent and incoherent  $\rho^0$  production, which is in agreement with theoretical calculations that include the effect of color transparency. The first-order intensity density for exclusive electroproduction of  $\pi^+\pi^-$  pairs has been studied as a function of the invariant mass  $M_{\pi\pi}$  in the range  $0.3 < M_{\pi^+\pi^-} < 1.5$  GeV. The derived quantities show a dependence of the  $\pi^+\pi^-$  invariant mass, which can be understood as due to the interference between pion pairs in relative P-wave (isovector channel) and S,D-waves (isoscalar channel) states.

PACS numbers: 25.30.-c, 13.60.Le, 21.30.Fe

UDC 539.12

Keywords: resonant and non-resonant  $\pi^+\pi^-$  pairs, cross sections, hard exclusive electroproduction, generalized parton distributions

## 1. Introduction

Our understanding of the quark–gluon dynamics can be extended considerably if information could be obtained on the recently re-introduced generalized parton distributions (GPDs) [1, 2], which take into account dynamical correlations between partons with different momenta. Experimentally, GPDs can be investigated in hard exclusive production of mesons or non-resonant pion pairs by longitudinally-polarized virtual photons. Under these conditions, the amplitude factorizes into a

hard part governed by perturbative QCD, a meson (or pion pair) distribution amplitude, and a soft part given by the GPDs [3]. In Ref. [3], the QCD factorization theorem was proven. It is of interest to note that according to Ref. [4], the theorem is related to the onset of color transparency.

One of fundamental predictions of QCD is the existence of the phenomenon called color transparency (CT). Its characteristic feature is that, at sufficiently high squared four-momentum transfer ( $-Q^2$ ), the initial- and final-state interactions of a hadron traversing a nuclear medium vanish [5–8]. The idea is that the dominant amplitudes for exclusive reactions at high  $Q^2$  involve hadrons of reduced transverse size, and that these small color-singlet objects, or small size configurations (SSC), have reduced interaction cross section with hadrons in the surrounding nuclear medium. Moreover, it needs to be assumed that these SSC remain small long enough when traversing the nucleus.

Additional information on GPDs can be obtained from hard exclusive electroproduction of  $\pi^+\pi^-$  pairs. This process is sensitive to the interference between the two isospin channels involved and thus provides a unique window on the quantum mechanical structure of the pion pair produced. In order to study the interference between  $\pi^+\pi^-$  production in P-wave and S,D-wave states ( $I = 1$  and  $I = 0$ , respectively), the intensity densities  $\langle P_1(\cos\theta) \rangle$  and  $\langle P_3(\cos\theta) \rangle$  are evaluated as a function of the pion pair invariant mass  $M_{\pi\pi}$ , and the Bjorken scaling variable  $x = Q^2/(2\nu M_p)$ , where  $M_p$  is the proton mass and  $\nu$  is the virtual photon energy. The quantity  $\langle P_n(\cos\theta) \rangle$  is the  $n^{\text{th}}$ -order Legendre polynomial of  $\cos\theta$  weighted by the differential cross section, and is also often referred to as the  $P_n(\cos\theta)$  moment

$$\langle P_n(\cos\theta) \rangle^{\pi^+\pi^-} = \frac{\int_{-1}^1 d\cos\theta P_n(\cos\theta) \frac{d\sigma^{\pi^+\pi^-}}{d\cos\theta}}{\int_{-1}^1 d\cos\theta \frac{d\sigma^{\pi^+\pi^-}}{d\cos\theta}},$$

with  $\theta$  being the production angle of the  $\pi^+$  meson with respect to the recoiling target direction in the  $\pi^+\pi^-$  center of mass system. Moreover, it can be shown that [9]

$$\frac{d\sigma^{\pi^+\pi^-}}{d\cos\theta} \propto P_l \cdot P_{l'},$$

with  $P_{l(l')}$  describing the angular state of the produced  $\pi^+\pi^-$  channel with total angular momentum quantum number  $J = l(l')$ . Using the orthonormal properties of Legendre polynomials, it can be shown that  $\langle P_n(\cos\theta) \rangle$  vanishes when the following two conditions are satisfied:  $n$  is odd and the interference term of the amplitude is absent. In particular,  $\langle P_1(\cos\theta) \rangle$  is sensitive to the interference between pion pairs in P-wave and S,D-wave states, while  $\langle P_3(\cos\theta) \rangle$  is sensitive to the interference between  $\pi^+\pi^-$  pairs in P-wave and in D-wave states only.

## 2. Data selection

The data sample used for the present analysis was extracted from events with exactly three tracks: a scattered positron and two oppositely charged hadrons, as described in detail in Ref. [10]. Events with  $\pi^0$  mesons were excluded by disregarding events with an untracked cluster in the calorimeter. For each event were evaluated  $x$ , the squared four-momentum transfer to the target  $t' = t - t_0$ , with  $t_0$  its minimum value, and the photon-nucleon invariant mass squared  $W^2 = M_p^2 + 2M_p\nu - Q^2$ . The kinematic coverage in  $\nu$ ,  $x$  and  $W$  is  $5 < \nu < 24$  GeV,  $0.01 < x < 0.35$  and  $3 < W < 6.5$  GeV, with mean values of 13.3 GeV, 0.07 and 4.9 GeV, respectively.

The exclusive  $\pi^+\pi^-$  production signal was extracted from the data in the kinematic region  $-2 < \Delta E < 0.6$  GeV, where  $\Delta E = \nu - E_\rho + t/(2M_p)$  is the exclusivity variable [10,11] with  $E_\rho$  the energy of the produced  $\rho^0$  meson, and  $M_{\pi\pi}$  the invariant mass of the detected hadron pair, assuming that they were pions. The subsample for exclusive  $\rho^0$  production was obtained by requiring  $0.6 < M_{\pi\pi} < 1.0$  GeV. In the study of nuclear transparency for exclusive  $\rho^0$  production, the  $\rho^0$  mesons have been selected by imposing  $|t'| < 0.045$  GeV<sup>2</sup> for nitrogen and  $|t'| < 0.4$  GeV<sup>2</sup> for hydrogen in the coherent case, while in the analysis of the incoherent  $\rho^0$  production a  $t'$  restriction was used for both data samples  $0.09 < |t'| < 0.4$  GeV<sup>2</sup>. The non-exclusive background for hydrogen was estimated  $6 \pm 3\%$  [10]. In these analyses the resolution in  $\Delta E$  is about 0.25 GeV [11], while the  $t'$  resolution is about 0.008 GeV<sup>2</sup>. It has been shown [10] that the incoherent  $t'$  slope parameter  $b_p$  for various nuclei is consistent with the hydrogen value  $b_p = (7.08 \pm 0.3)$  GeV<sup>-2</sup>. The coherent slope parameter on nitrogen,  $b_{^{14}\text{N}} = (57.2 \pm 3.3)$  GeV<sup>-2</sup>, is in agreement with the values predicted by the relationship  $b_A \approx R_A^2/3$  [10], where  $R_A$  is the nuclear radius.

## 3. Coherence length effect

For the incoherent  $\rho^0$  production, the nuclear transparency has been evaluated using the expression  $T_{\text{inc}} = \sigma_{\text{inc}}^A / (A\sigma_p) = N_{\text{inc}}^A \mathcal{L}_p / (AN_p \mathcal{L}_A)$  [10], where p refers to <sup>1</sup>H, A to <sup>14</sup>N,  $N_{\text{inc}}^A$  is the number of incoherent events,  $N_p$  the number of events on <sup>1</sup>H, and  $\mathcal{L}_{A,p}$  is the effective luminosity of the nitrogen or hydrogen samples, corrected for detector and reconstruction inefficiencies. In addition, a ‘‘Pauli blocking’’ correction has been applied, which accounts for the absence of incoherent  $\rho^0$  production on nitrogen at momentum transfers  $|t'|$  smaller than the nuclear Fermi momentum.

For the coherent  $\rho^0$  production, the quantity  $T_c = \sigma_c^A / (A\sigma_p)$  is evaluated. The quantity  $\sigma_c^A$  has also been corrected for the different  $t'$  requirements that were applied to the nitrogen and the hydrogen data. Moreover, corrections have been applied for the acceptance differences caused by the different  $t'$  regions selected, as evaluated from Monte Carlo simulations of exclusive  $\rho^0$  production in a  $4\pi$  geometry and in the HERMES acceptance [11], and differences in the radiative correction factors [12] for nitrogen and hydrogen.

The nuclear transparencies for coherent and incoherent  $\rho^0$  production are presented in the left panel of Fig. 1 [13] as functions of the coherence length

$$l_c = \frac{2\nu}{Q^2 + M_{\pi\pi}^2},$$

a propagation distance of  $q\bar{q}$  fluctuation of the virtual photon evolved on-shell to  $\rho^0$  meson. The data for incoherent  $\rho^0$  production supersede the previously published data [10], as the present analysis includes ‘‘Pauli blocking’’ corrections and makes use of a fixed requirement on  $t'$  over the entire coherence length region. The data decrease with increasing  $l_c$ , as expected from the effect of initial-state interactions.

The nuclear transparency for coherent  $\rho^0$  production is seen to increase with coherence length, which can be attributed to the momentum-transfer dependence of the nuclear form factor [8]. Good agreement is found between the measured nuclear transparencies, integrated over the available  $Q^2$  region, and calculations including both the coherence length and CT effects [8] evaluated for each  $l_c$  bin at their mean experimental  $l_c$  and  $Q^2$  values, as given by the curves in the left panel of Fig. 1. The effect of the nuclear form factor on  $T_c$  is included in the calculations.

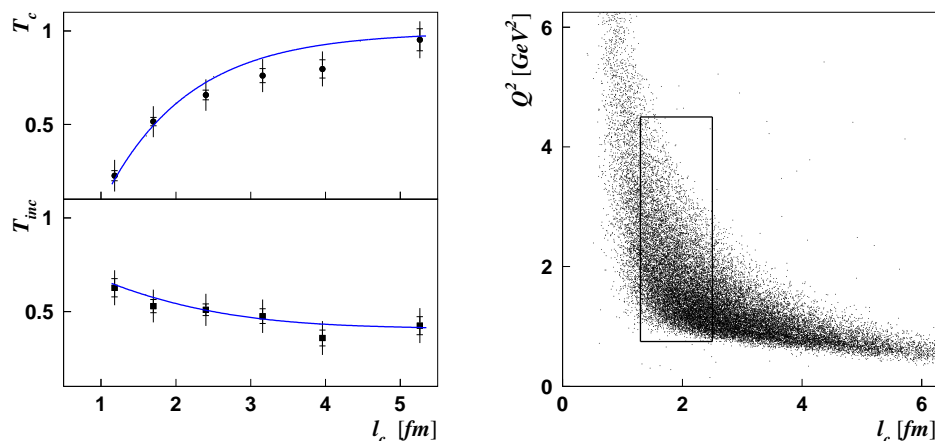


Fig. 1. Left panel: Nuclear transparency as a function of coherence length for coherent (top) and incoherent (bottom)  $\rho^0$  production on nitrogen, compared to predictions with CT effects included (curves) [8]. The inner error bars include only statistical uncertainties, while the outer error bars present the statistical and systematic uncertainties added in quadrature. Right panel: Distribution of  $Q^2$  versus coherence length for exclusive  $\rho^0$  production on hydrogen and nitrogen. The region surrounded by the rectangle represents the subset that was used for the two-dimensional analysis of the nuclear transparency.

#### 4. Color transparency effect

A two-dimensional analysis of the nuclear transparency as a function of coherence length and  $Q^2$  has been performed, which represents a new approach in the

search for CT. The idea is to deconvolute the effect of CT and the coherence length by evaluating the  $Q^2$ -dependence of the data for very narrow  $l_c$  bins such that the coherence length effect is constant. In order to identify the kinematical domain best suited for this search, the range in  $Q^2$  and  $l_c$  covered by the present data is shown in the right panel of Fig. 1. The statistical significance and the  $Q^2$  coverage is seen to be largest near  $l_c \simeq 2.0$  fm. For that reason the region  $1.3 < l_c < 2.5$  fm has been chosen for this two-dimensional analysis. Coherence length bins of 0.1 fm were used. These finite bins introduce an additional systematic uncertainty in the  $Q^2$ -slope of 0.008 and 0.004  $\text{GeV}^{-2}$  for coherent and incoherent  $\rho^0$  production, respectively. In order to extract the  $Q^2$ -dependence, each  $l_c$  bin was independently split into 3 or 4  $Q^2$  bins.

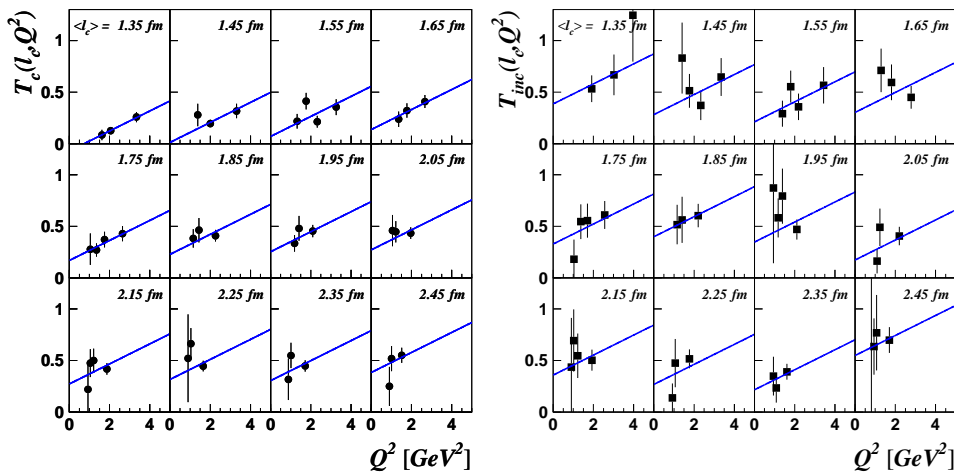


Fig. 2. Nuclear transparency as a function of  $Q^2$  in specific coherence length bins (as indicated in each panel) for coherent (left panel) and incoherent (right panel)  $\rho^0$  production on nitrogen. The straight line is the result of the common fit of the  $Q^2$ -dependence. The error bars include only statistical uncertainties.

The nuclear transparency was determined in each  $(l_c, Q^2)$  bin, and, as shown in Fig. 2, for twelve  $l_c$  bins both for the coherent and incoherent  $\rho^0$  production. The low statistics in each  $(l_c, Q^2)$  bin makes it difficult to fit the slope of the  $Q^2$ -dependence for each coherence length bin separately. Instead, the data have been fitted with a common  $Q^2$ -slope ( $P_1$ ), which has been extracted assuming

$$T_{c(\text{inc})} = \sigma_{c(\text{inc})}^{14\text{N}}(l_c, Q^2)/A\sigma_p = P_0 + P_1 \cdot Q^2,$$

letting  $P_0$  vary independently in each  $l_c$  bin and keeping  $P_1$  as a common free parameter. The results of the combined fit are displayed as solid lines in Fig. 2 [13]. For both the coherent and the incoherent data, the reduced- $\chi^2$  value is close to unity. The common  $Q^2$ -slope parameter,  $P_1$ , represents a possible signature of the CT effect averaged over the covered coherence length range. This procedure was

performed separately for the coherent and incoherent data. The  $Q^2$ -slope was found to vary by at most 17% (20%) for the coherent (incoherent) data when shifting the  $l_c$  window used in the fit from 1.0–2.2 fm to 1.4–2.6 fm. This variation is treated as an additional systematic uncertainty. If the results are combined, the common value for the  $Q^2$ -slope for exclusive  $\rho^0$  production is  $(0.074 \pm 0.023) \text{ GeV}^{-2}$  [13]. This is in agreement with the combined theoretical prediction of about  $0.058 \text{ GeV}^{-2}$  [8].

### 5. Exclusive non-resonant $\pi^+\pi^-$ production

In Fig. 3, the preliminary HERMES results on the  $M_{\pi\pi}$ -dependence of the intensity density  $\langle P_1(\cos\theta) \rangle$  are shown, for the proton in the left panel and the deuteron in the right one. The distributions show a non-zero  $P_1(\cos\theta)$  moment, the size of which changes with  $M_{\pi\pi}$ . At low  $M_{\pi\pi}$  ( $M_{\pi\pi} < 0.6 \text{ GeV}$ ), the asymmetry is possibly due to an interference between the lower tail of the  $\rho^0$  meson and non-resonant  $\pi^+\pi^-$  S-wave production ( $I = 1$  and  $I = 0$  interference). This interference is present over the entire invariant mass region considered. At large  $M_{\pi\pi}$  ( $M_{\pi\pi} > 1.0 \text{ GeV}$ ), additionally, an interference between the upper tail of the  $\rho^0$  meson and  $f$ -type mesons arises. In particular, the possible change of sign of the asymmetry near  $M_{\pi\pi} \approx 1.3 \text{ GeV}$  may be understood to be caused by the interference of the broad  $\rho^0$  tail and the  $f_2$  resonance (1.270 GeV).

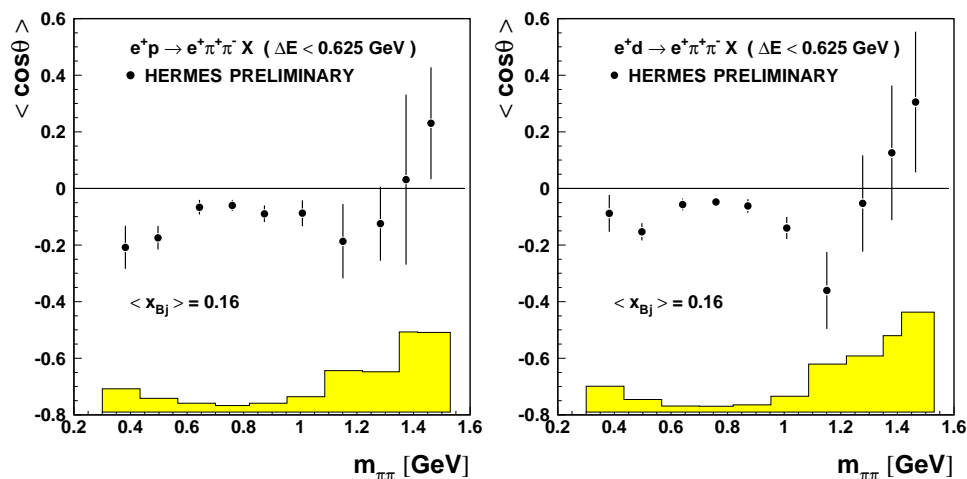


Fig. 3.  $M_{\pi\pi}$ -dependence of the intensity density  $\langle P_1(\cos\theta) \rangle$  for the proton (left panel) and the deuteron (right panel). Shaded areas in both panels represent the systematic uncertainty.

In the left panel of Fig. 4, the data are compared with theoretical calculations based on the GPD framework, with [9,14] and without [9] the inclusion of the two-gluon exchange mechanism for the  $M_{\pi\pi}$ -dependence of  $\langle P_1(\cos\theta) \rangle$ . In the calculations, a possible contribution of the  $f_0$  meson was not considered. Predictions

based on only using the quark exchange mechanism in the GPD framework [14], are compared with data for the  $x$ -dependence of  $\langle P_1(\cos\theta) \rangle$  in the right panel of Fig. 4. It is noted that these GPD calculations only include the longitudinal component  $\sigma_L$  of the  $\pi^+\pi^-$  cross section, while in this analysis no separation between the  $\sigma_L$  and  $\sigma_T$  contributions was made. Very roughly, the  $\sigma_T$  contribution can be estimated as  $\sim 50\%$  [11]. Nevertheless, the calculations succeed in giving a fair account of the gross features of the data.

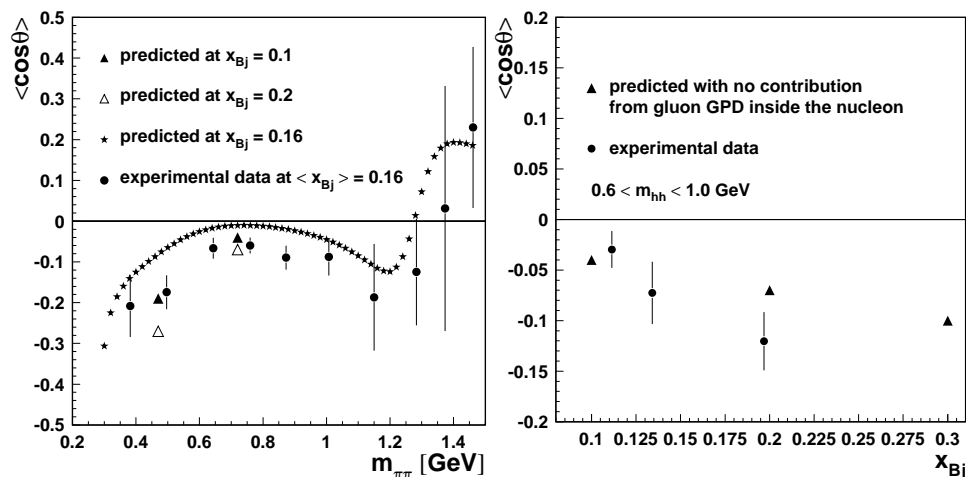


Fig. 4. The experimental  $M_{\pi\pi}$ -dependence (left panel) and  $x_{Bj}$ -dependence (right panel) of the intensity density  $\langle P_1(\cos\theta) \rangle$  for the proton are compared with theoretical predictions from Refs. [9] and [14]. Triangles (stars) show the predictions with the gluon GPD neglected [14] (included [9]). In the left panel, the triangles have been slightly shifted for a better visibility.

## 6. Summary

The intensity density  $\langle P_1(\cos\theta) \rangle$  for exclusive electroproduction of  $\pi^+\pi^-$  pairs has been measured for the first time, for hydrogen and deuterium targets separately. The data show signatures of the interference between pion pairs in the isospin states  $I = 1$  (P-wave) and  $I = 0$  (S, D-wave).

### Acknowledgements

I wish to thank my colleagues in the HERMES collaboration and A. Airapetian and R. Fabbri for useful discussions and suggestions in particular.

## References

- [1] A. V. Radyushkin, Phys. Rev. D **56** (1997) 5524.
- [2] X. Ji, J. Phys. G **24** (1998) 1181.
- [3] J. Collins, L. Frankfurt and M. Strikman, Phys. Rev. D **56** (1997) 2982.
- [4] M. Strikman, Nucl. Phys. A **663–664** (2000) 64.
- [5] A. B. Zamolodchikov et al., Pis'ma Zh. Eksp. Teor. Fiz. **33** (1981) 612; Sov. Phys. JETP Lett. **33** (1981) 595.
- [6] G. Bertsch et al., Phys. Rev. Lett. **47** (1981) 297.
- [7] S. J. Brodsky and A. H. Mueller, Phys. Lett. B **206** (1988) 685.
- [8] B. Z. Kopeliovich et al., Phys. Rev. C **65** (2002) 035201; B. Z. Kopeliovich and J. Nemchik, private communication.
- [9] B. Lehmann-Dronke et al., Phys. Rev. D **63** (2001) 114001.
- [10] K. Ackerstaff et al., HERMES Collaboration, Phys. Rev. Lett. **82** (1999) 3025.
- [11] A. Airapetian et al., HERMES Collaboration, Eur. Phys. J. C **17** (2000) 389.
- [12] I. Akushevich, Eur. Phys. J. C **8** (1999) 457.
- [13] A. Airapetian et al., HERMES Collaboration, Phys. Rev. Lett. **90** (2003) 052501.
- [14] B. Lehmann-Dronke et al., Phys. Lett. B **475** (2000) 147.
- [15] M. Garcon, hep-ph/0210068, to be published in Eur. Phys. Jour. A.

TVRDA EKSKLUZIVNA ELEKTROTIVORBA REZONANTNIH I  
NEREZONANTNIH PAROVA PIONA U HERMESU

Predstavljamo odabir ishoda nedavnih mjerenja tvrde ekskluzivne elektrotvorbe rezonantnih i nerezonantnih parova  $\pi^+\pi^-$ . Nalazimo da omjer udarnih presjeka elektrotvorbe  $\rho^0$  po nukleonu u  $^{14}\text{N}$  i  $^1\text{H}$ , poznat kao nuklearna prozirnost, raste (opada) s povećanjem koherentne duljine za koherentnu (nekoherentnu) elektrotvorbu. Za određenu koherentnu duljinu, opaža se porast sa  $Q^2$  za koherentnu kao i za nekoherentnu tvorbu  $\rho^0$ , što je u skladu s teorijskim računima koji uključuju učinke prozirnosti boje. Proučavali smo gustoću intenziteta za ekskluzivnu elektrotvorbu parova  $\pi^+\pi^-$  u prvom redu, kao funkciju invarijantne mase  $M_{\pi\pi}$  u području  $0.3 < M_{\pi^+\pi^-} < 1.5$  GeV. Izvedene veličine pokazuju ovisnost invarijantne mase  $\pi^+\pi^-$ , što se može shvatiti posljedicom interferencije među pionskim parovima u relativnim P-valnim (izovektorski kanal) i S,D-valnim stanjima (izoskalarni kanal).